

# Histological And Immunochemical Studies of The Possible Protective Role of Riboflavin and Urolithin A on Carbon Tetrachloride-Induced Hepatotoxicity in Albino Rats

Samar Fawzy Gad<sup>1</sup>, Maged Behery<sup>1</sup>

<sup>1</sup>Department of Anatomy and Embryology, Faculty of Medicine, Benha University, Benha 13518, Egypt

\*Corresponding author: Samar Fawzy Gad, Mobile: (+20) 01067490565, E-Mail: samar.gad@fmed.bu.edu.eg

## ABSTRACT

**Background:** Carbon Tetrachloride is used as a dry-cleaning solvent and in lava lamps. Previous research has demonstrated its harmful potential for several organs. **Aim:** The objective of the current work is to examine any hepatoprotection induced by Riboflavin, Urolithin A, and combined Riboflavin and Urolithin A on an animal model of liver damage brought by CCl<sub>4</sub>. Histological and immunohistochemical investigations were also used to study the processes behind such protection. **Material and methods:** Five equal groups of forty Wistar albino rats were created. In this study, Wistar rats were given CCl<sub>4</sub> intraperitoneally (1 mL/Kg bw) on day 7 as a single dose while given riboflavin by oral gavage, Urolithin A intraperitoneally and combined Riboflavin and Urolithin A for 14 days. After the experiment, blood samples were obtained to measure the liver enzymes. Liver samples were prepared using Masson trichrome as well as Hematoxylin and Eosin staining. Bax and Bcl2 immunoexpression were detected.

**Results:** Along with disturbed architecture and vacuolization of hepatocytes shown in the H & E results linked with fibrous propensity in the Masson- trichrome samples, CCl<sub>4</sub>-exposed animals demonstrated significant disruption of the biochemical tests. In the group receiving either riboflavin or/and urolithin A, the histology and biochemical markers were adjusted after therapy.

**Conclusion:** Through elevation of anti-apoptotic proteins and suppressing of pro-apoptotic proteins, riboflavin and/or urolithin A protected against CCl<sub>4</sub>-induced liver damage. Together, they had a synergistic effect.

**Keywords:** Carbon tetrachloride, Riboflavin, Urolithin A, Bax, Bcl2.

## INTRODUCTION

The liver is the first organ to be affected by the noxious effects of freshly produced toxic chemicals. There continues to be evidence that reactive oxygen species and free radicals are essential for many processes that initiate and control the development of liver diseases <sup>(1)</sup>. Carbon tetrachloride (CCl<sub>4</sub>) is a colourless, non-flammable liquid formed by the reaction of chlorine with chloroform in the presence of light. It is a widely used chemical solvent in industry, as well as a cleaning agent and degreaser in the household. It is classified as an environmental contaminant that causes tissue necrosis and cell damage <sup>(2)</sup>. CCl<sub>4</sub> caused toxicity by producing the free radical trichloromethyl (CCl<sub>3</sub><sup>\*</sup>) and other cytochrome P450 metabolites. This radical attaches to cellular molecules (nucleic acid, protein, lipid), affecting cellular functions and resulting in fatty degeneration, whilst the interaction between CCl<sub>3</sub><sup>\*</sup> and DNA is hypothesised to operate as a liver cancer initiator. This radical can also combine with oxygen to create the extremely reactive trichloromethylperoxy (CCl<sub>3</sub>OO<sup>\*</sup>) radical. Finally, CCl<sub>4</sub> poisoning causes lipid peroxidation in mitochondrial, endoplasmic reticulum, and other key organelle membranes, resulting in inflammation and cellular death by apoptosis or necrosis <sup>(3)</sup>.

CCl<sub>4</sub> poisoning is a complex process in which any antioxidant or anti-inflammatory characteristics may be beneficial to medical care. Riboflavin (Vitamin B<sub>2</sub>) is a water soluble vitamin. It is an important vitamin because of its function in macromolecule metabolism in all living organisms. Flavin adenine dinucleotide (FAD) and flavin adenine mononucleotide (FMN) are its two

coenzymatic forms in biological systems. About 100 distinct metabolic redox activities, including those related to stress response, body development and DNA repair, are carried out by these flavin proteins in all forms of life <sup>(4)</sup>. Riboflavin's antioxidant action (as a cofactor for enzymes and as a regulator of gene expression) may have positive therapeutic effects. For example, enhanced histopathology results in renal toxicity <sup>(5)</sup>, acute lung injury <sup>(6)</sup> and ulcerative colitis <sup>(7)</sup>.

Naturally occurring polyphenols known as urolithins are created by the gut microbiota in response to ellagic acid (EA) and ellagitannins (ETs) -rich meals <sup>(8)</sup>. Recently, it was shown that Urolithin A promotes mitophagy in two distinct models of age-related muscular dystrophy <sup>(9)</sup>. Due to its strong antioxidant activity, urolithin A may play a significant part in protecting against various clinical disorders caused by oxidative stress on numerous organs, as the heart, liver, and kidney <sup>(8,10)</sup>. This study's objectives were to analyze the impact of carbon tetrachloride over rats' liver and the potential protective effects of riboflavin and urolithin A using biochemical, histological, immunohistochemical, and morphometric methods.

## MATERIAL AND METHODS

### Materials:

Carbon tetrachloride (cat. No.319961, purity >99%) was purchased from Sigma-Aldrich, Chemie GmbH as liquid solution.

Riboflavin (cat. No. 555682, purity >99%) was also procured from Sigma-Aldrich, Chemie GmbH. The Solution was prepared in saline immediately before the experiment by measuring out the desired amount of

riboflavin powder<sup>(11)</sup>. Urolithin A (cat. No. SML1791, purity >99%) was also purchased from Sigma-Aldrich, Chemie GmbH. To prepare UA solution, the compound was dissolved in sterilized PBS containing 5% dimethyl sulfoxide (DMSO, Sigma-Aldrich) at a concentration 20 mg/ml and stored in darkness at 4 °C. Suitable volume was collected from the stock solution and diluted in PBS to the required concentration for each animal just before intraperitoneal administration<sup>(12)</sup>.

**Animal:** Forty Wistar albino rats, weighed 180±20 g (10–12 weeks old), were obtained from the experimental animal farm (Helwan, Cairo, Egypt). They were kept on a conventional pellet food and water throughout the entire study under optimal laboratory circumstances (12 h light/12 h darkness cycle, temperature 23–25 °C).

### Experimental design

In five groups of eight animals each, the animals were randomly divided into:

**Group 1 (Control group):** two rats injected intra-peritoneal (i.p.) with an equal amount of olive oil single dose at the seventh day of study, two rats given an equal amount of normal saline by oral gavage and two rats administered (i.p.) with an equal amount of 5% DMSO/PBS liquid (as a vehicle); for 14 days.

**Group 2 (CCl<sub>4</sub> group):** On the seventh day, in addition to their regular feed and water, rats received an intraperitoneal (i.p.) injection of 1 mL/Kg body weight of carbon tetrachloride that was dissolved in an equivalent amount of olive oil (1:1 v/v ratio)<sup>(1)</sup>.

**Group 3: (CCl<sub>4</sub> treated with Riboflavin group)** rats were administered CCl<sub>4</sub> intraperitoneally (1 mL/Kg) on the seventh day while given riboflavin by oral gavage (100 mg/kg bw) daily for 14 days<sup>(13)</sup>.

**Group 4: (CCl<sub>4</sub> treated with UA group)** rats were administered CCl<sub>4</sub> intraperitoneally (1 mL/Kg bw) on day 7 while given Urolithin A intraperitoneally (5 mg/Kg bw) daily for 14 days<sup>(12)</sup>.

**Group 5: (CCl<sub>4</sub> treated with Riboflavin and UA group)** rats were administered CCl<sub>4</sub> intraperitoneally (1 mL/Kg bw) on day 7 while given riboflavin by gavage (100 mg/kg bw) and Urolithin A intraperitoneally (5 mg/Kg bw) daily for 14 days. All rats were decapitated while receiving intramuscular xylazine -ketamine anaesthesia 24 hours following the final dose of the prescribed therapy. The livers were immediately eliminated and properly cleansed at ice-cold saline after the abdomen was longitudinally sliced to obtain blood samples from the heart. Following that, the removed livers were dried using Whatman filter paper. Liver slices were preserved for further histological examination in a 10% neutral formalin solution.

**Biochemical tests:** The blood sample was obtained and centrifuged in a centrifuge tube that had been heparinized. Plasma samples were analysed spectrophotometrically to evaluate the levels of alanine aminotransferase enzyme (ALT) [ab285264, abcam]

and aspartate aminotransferase enzyme (AST) [ab263883, abcam].

**Histological examination:** Hepatic tissue samples were fixed in 10% formaldehyde solution and embedded in paraffin. The 5 µm thick sections were stained stained with hematoxylin and eosin (H&E) and Masson's Trichrome<sup>(14)</sup>.

### Immunohistochemistry assay

The current investigation used xylene and alcohol to deparaffinize and rehydrate Bax and Bcl-2 immunoreactivity. The sections were then washed with distilled water before being placed in a microwave with citrate buffer (10 mmol/L) for twenty minutes. 1% H<sub>2</sub>O<sub>2</sub> was then applied to the sections for twenty minutes, followed by ten minutes of a protein block fluid from Dako, Carpinteria, California. The rat monoclonal antibody against Bcl-2 Antibody (EP10625, abcam) and Bax (AB81083, abcam) in 1:50 was used for 90 minutes to specific of Bcl-2 and Bax proteins. Finally, the peroxidase reaction was started with 3, 3'diaminobenzidine tetra-hydrochloride (Sigma), and the secondary stain was hematoxylin.<sup>(15)</sup>

The hepatic sections were captured using a Toupcam™ Xcam full HD camera and a Nikon Eclipse 80i light microscope (Nikon Corporation, Japan) in Anatomy Department, the Faculty of Medicine at Benha University in Egypt.

**Morphometric study:** An expert who was not aware of the research groups conducted the image analysis. JPG file format photomicrographs were collected, and image analysis was performed through VideoTesT-Master software from the Argussoft Ltd. firm in Saint Petersburg, Russia. BAX and Bcl-2 expression levels were measured using mean integrated optical density at x400 magnification.

**Ethical approval:** The experiment was carried out at Anatomy department at Benha University's Faculty of Medicine in accordance with the rules of the animal care and use Ethics Committee of the Faculty of medicine at Benha University (Approval No.: Rc.9.6.2023).

**Statistical analyses:** The data were analysed and the groups were compared using GraphPad prism, for Windows (San Diego, California, USA), one-way ANOVA, and post hoc Tukey's test in accordance with the research design. The outcomes are shown as mean SD. An additional criterion for statistical significance was a p value greater than 0.05.

### RESULT

**Biochemical tests:** When compared to control values, the biochemical examination of liver enzymes showed an obvious increase ( $p < 0.05$ ) in ALT and AST in the CCl<sub>4</sub> group. In comparison to the CCl<sub>4</sub>-group, single treatments with Riboflavin or UA, as well as both Riboflavin/UA combinations, exhibited an obvious decrease ( $p < 0.05$ ) in blood levels of liver enzymes (Table 1, Fig. 1).

**Table (1): Comparison of Serum level of liver enzymes between different groups**

Mean % ± SD	Group I	Group II	Group III	Group IV	Group IV
AST	25.5 ± 1.1 <sup>P</sup>	154.2 ± 8.1 <sup>c,R,U&amp;T</sup>	27 ± 0.95 <sup>P</sup>	30.8 ± 1.9 <sup>P</sup>	29 ± 1 <sup>P</sup>
ALT	17.3 ± 0.7 <sup>P</sup>	56.5 ± 3.5 <sup>c,R,U&amp;T</sup>	18.9 ± 0.85 <sup>P</sup>	18.8 ± 1.1 <sup>P</sup>	18.5 ± 1.1 <sup>P</sup>

The value of groups is presented as mean±SD.: significance <0.05.

c: Significance vs group I, p: Significance vs group II, R: Significance vs group III, U: Significance vs group IV, T: Significance vs group V.

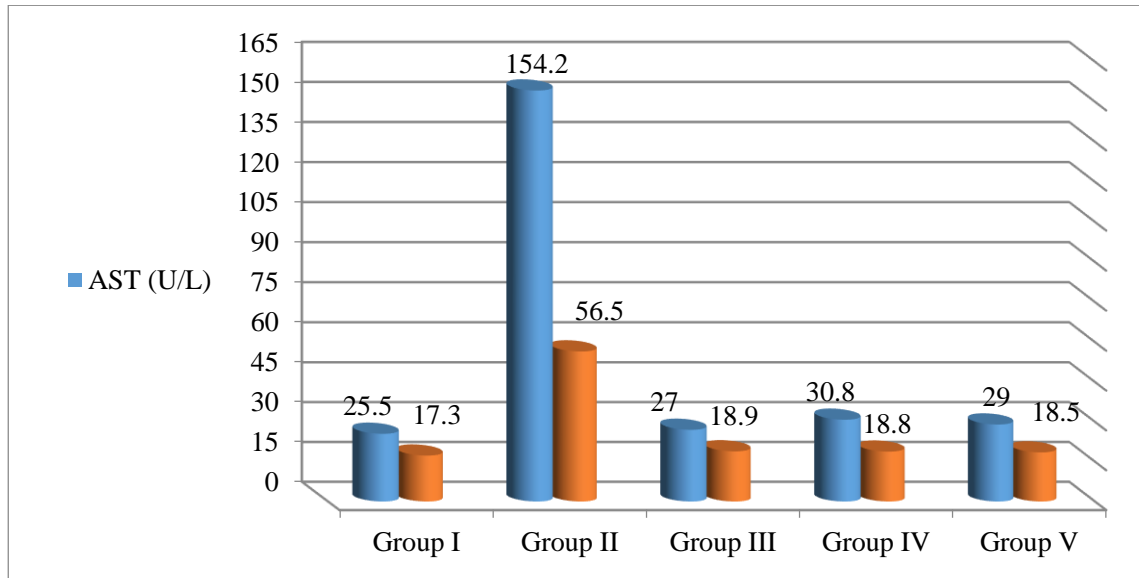


**Fig. (1): Comparison of Serum level of liver enzymes between different experimental groups.**

**Hematoxylin and Eosin staining:**

**Group I**

Hepatic lobules with a typical form of around a hexagon and central veins indicating their center axis were seen in liver slices from the Control group. Hepatocytes with large nucleoli and rounded vesicular nuclei with acidophilic cytoplasm formed composed each typical hepatic lobule. They were arranged in polygonal anatomizing cords. Blood sinusoids were discovered as a network between Kupffer cells and flattened endothelial cells lining the hepatocytes between the radiating plates (fig. 2A). There were portal areas with connective tissue stroma at their angles. It contained a bile ductule, a terminal branch of the hepatic artery, and a tiny branch of the portal vein. (fig.2B ).

**Group II**

This group's liver sections revealed degenerative alterations in the form of disrupted hepatic architecture, congested central veins, and dilated blood sinusoids. The majority of the hepatocytes were necrotic with cytoplasmic vacuolization, with variable sized vacuoles. Furthermore, there were some nuclear alterations seen, including pyknotic nuclei with dark staining, karyorrhexis, and karyolysis. Additionally, nuclear vacuolations in hepatocytes were seen (fig. 3A).

There were severe cellular infiltrations in the portal area (fig.3B).

**Group III**

Liver sections of this group revealed dilatation and of the central veins and blood sinusoids. Some of the hepatocytes apparently normal and few cells are showed cytoplasmic vacuoles (fig. 4A). Moderate cellular infiltrations were found around a portal area's components (fig.4B).

**Group IV**

Liver sections of this group showed mild dilatation of blood sinusoids. A majority of the hepatocytes had restored cytoplasm, with just a small number of cells having cytoplasmic vacuoles. (fig. 5A). Components of a portal area had mild cellular infiltrations. (fig.5B).

**Group V**

The hepatic tissue improvement was obvious in the liver sections of this group. Numerous areas under examination appeared to have a normal hepatic architecture without the infiltration of scattered inflammatory cells and without hepatocyte degeneration. (fig. 6A, B).

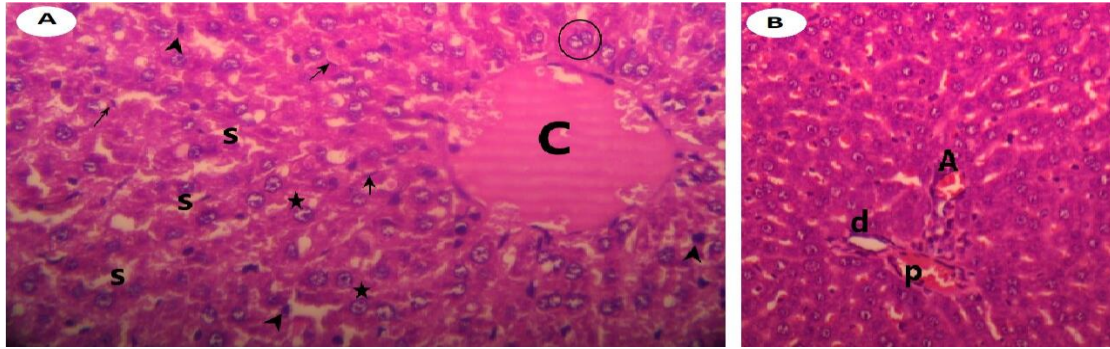


**Fig. (2):** A photomicrograph of the control group's liver sections showing the characteristic hepatic lobule: (A) has a central vein (c), hepatocytes, and blood sinusoids (S) which are bordered by Kupffer cells (head arrow) and flattened endothelial cells (arrow). Hepatocytes feature binucleated cells as well as big, spherical vesicular nuclei and prominent nucleoli (star). (H & E, X: 400). B) At the periphery of hepatic lobule, portal tract showing a portal venule (p), hepatic artery branches (A), and a bile duct (d). (H &E, X:200).

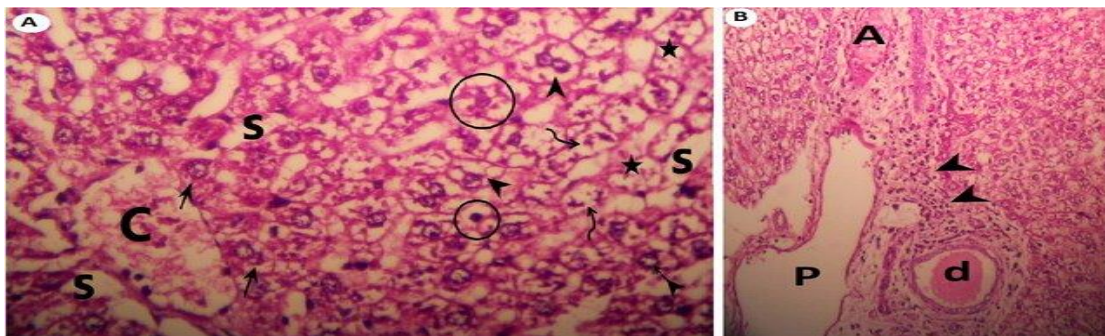


**Fig. (3):** A photomicrograph of liver section in Group II showing: (A) hepatic architecture disorganized, with congested central vein (C), and blood sinusoids (S). Hepatocytes feature a significant number of consolidated vacuoles (head arrow) or numerous tiny vacuoles (arrow). Some hepatocytes contain nuclei that are darkly stained (circle), fragmented (curved arrow), or lysed (star). Some hepatocytes contain nuclei that have vacuoles. (Bifid arrow). (H &E, X:400). (B) The portal tract's components, including branch of the hepatic artery (A), portal venule (p), and a bile duct (d), are surrounded by severe cellular infiltrations (head arrows). (H & E, X: 200).

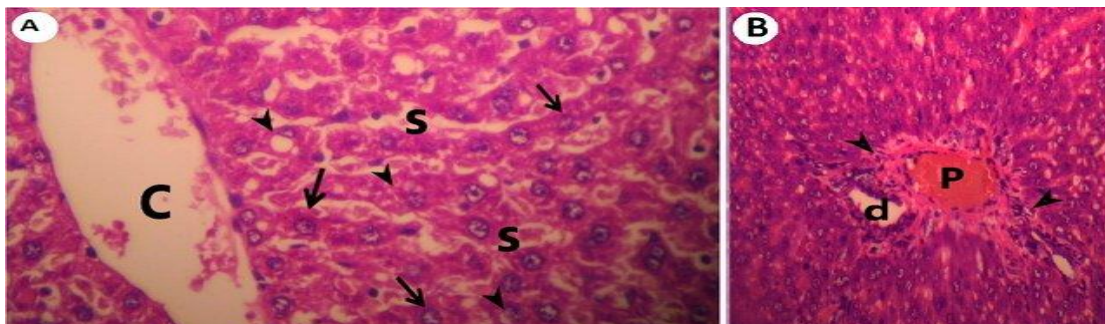


**Fig. (4):** Photomicrographs of liver sections in Group III showing: A) Blood sinusoids (S) and the central vein (C) are both dilated. There are number of hepatocytes that seem normal (arrow) and a few cells with cytoplasmic vacuoles (head arrow). (H &E, X:400). B) Seen here are a portal venule (p) and a bile ductile (d), all of which are surrounded by moderate cellular infiltrations (head arrow). (H &E, X:200).

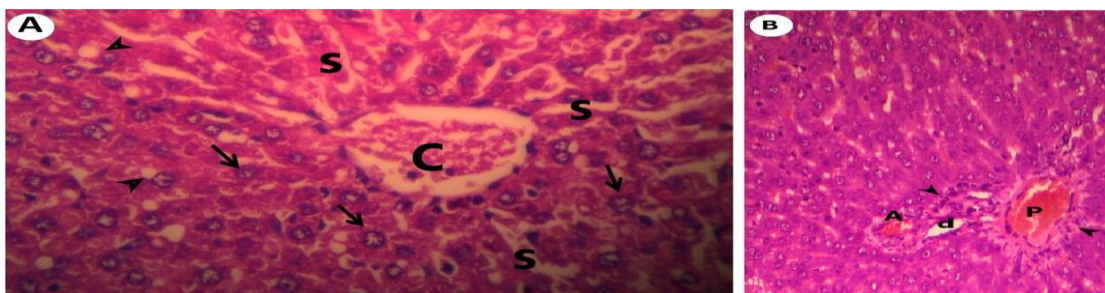


**Fig. (5):** Photomicrographs of liver sections in Group IV showing: (A) The majority of hepatocytes (arrow) seen surrounding central vein (C) are normal. Cytoplasmic vacuoles are observed in few cells (head arrow). Blood sinusoids (S) have a mild dilation. (H and E, X: 400). B) Notice a portal venule (p), branch of the hepatic artery (A) and a bile ductile (d), all of which are surrounded by mild cellular infiltrations (head arrow). (H &E, X:200).

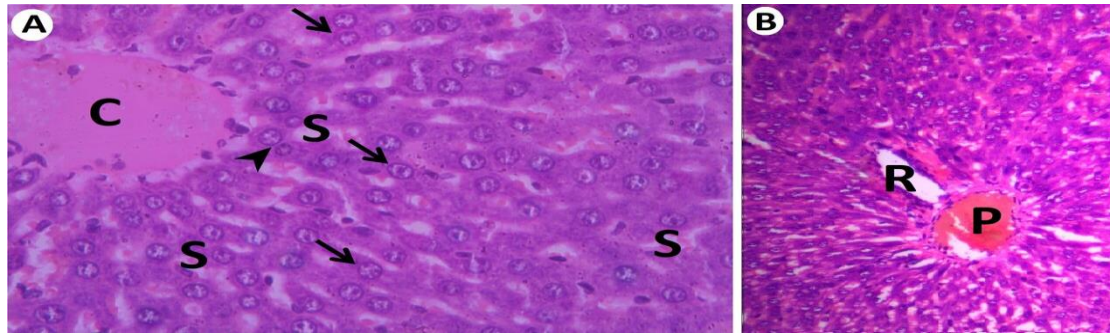


**Fig. (6): Photomicrographs of liver sections in Group V showing:**  
**(A) Normal hepatic lobular arrangement around apparently normal blood sinusoids (s) and the central vein (c). Round vesicular nuclei are found in hepatocytes (arrow), and some cells are also bi-nucleated (head arrow). (H and E, X:400). (b) Notice absence of cellular infiltrations surrounding the portal tract's structural elements reveals the hepatic artery (R) and bile duct (d) branches. (H &E, X:200).**

### Masson trichomats

One of the most often used special stains on liver materials for the assessment of fibrosis is the Masson's trichrome stain. Against a red background of hepatocytes and other structures, the dye gives collagen a blue hue. Type 1 collagen, which is present in portal tracts and vessel walls, is stained by it. <sup>(16)</sup>

Liver slices from rats in groups I, III, IV, and V stained with Mason trichrome revealed typical fibrous tissue deposition limited to the walls of central veins and blood vessels in portal areas, with no aberrant changes in fibrous tissue distribution. Collagen fibers were clearly distributed in the portal area of Group II liver sections (**fig.7A-F**).

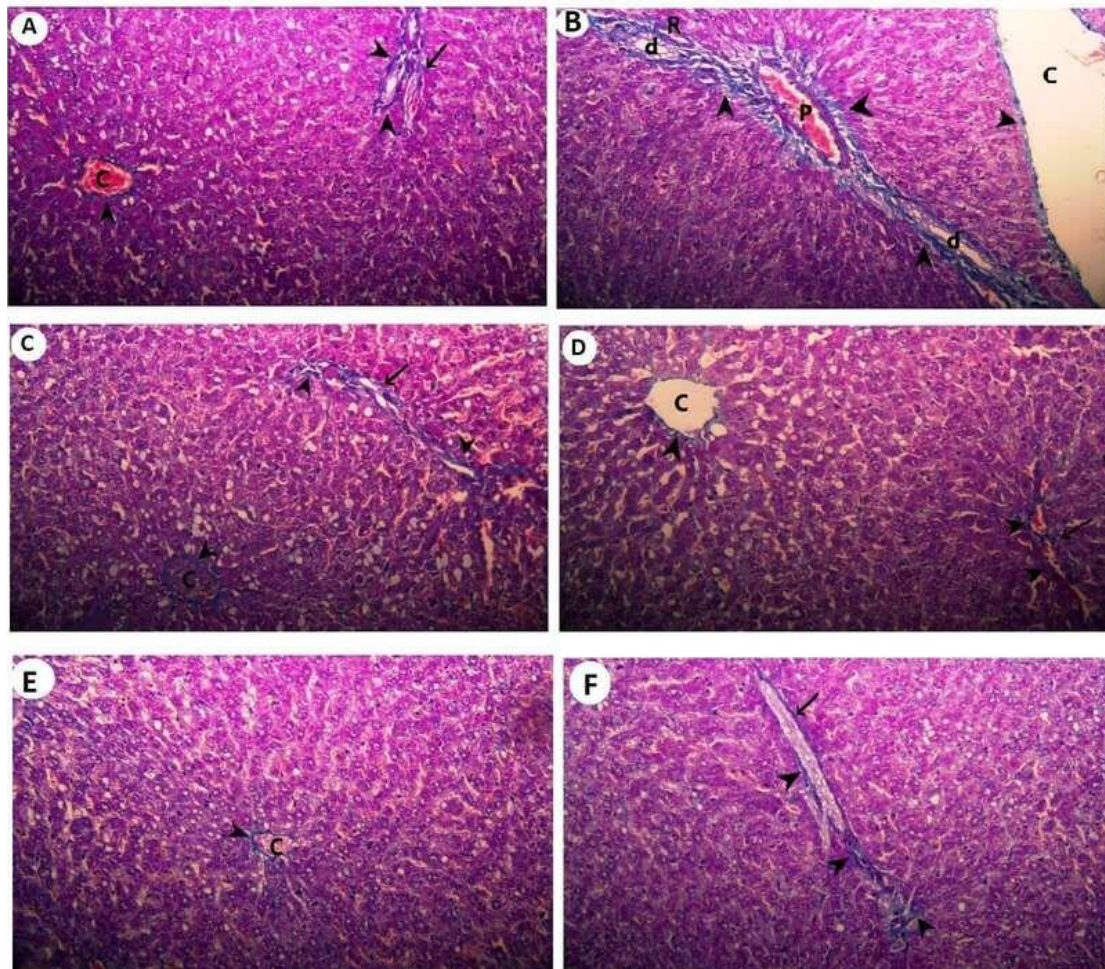


**Fig. (7) Masson-stained Photomicrographs of liver tissues in all rat groups,**  
**A, C and D represent group I, group III and group IV showing minimal collagen fibers (head arrow) surrounding the central veins (C) and in portal areas (arrow). (Masson's trichrome, X:200)**  
**E and F for group V showing minimal collagen fibers (head arrow) surrounding the central vein (V) and in portal area (arrow). (Masson's trichrome, X:200). B) group II showing increased amount of collagen fibers (head arrow) surrounding the contents of portal area including branch of portal vein (p), hepatic ductile (d) and branch of hepatic artery (R). (Masson's trichrome, X:200).**

## Bcl2

Hepatocytes' cytoplasm is stained with an anti-Bcl-2 antibody via immunohistochemistry <sup>(17)</sup>. The liver sections of group I observed strong expression of Bcl-2 proteins (Fig.8a). The weak expression was showed in the group II as compared to control group (Fig.8b).The liver tissues of group III and group IV showed moderate expression of Bcl-2 (Figs.8c,d) whereas strong expression of Bcl-2 proteins was observed in group V (Fig.8e). Liver tissues from rats of group I, III, IV and V showed a significant increase ( $p<0.05$ ) in the expression of Bcl-2 protein as compared to group II (table 2, Fig.9).

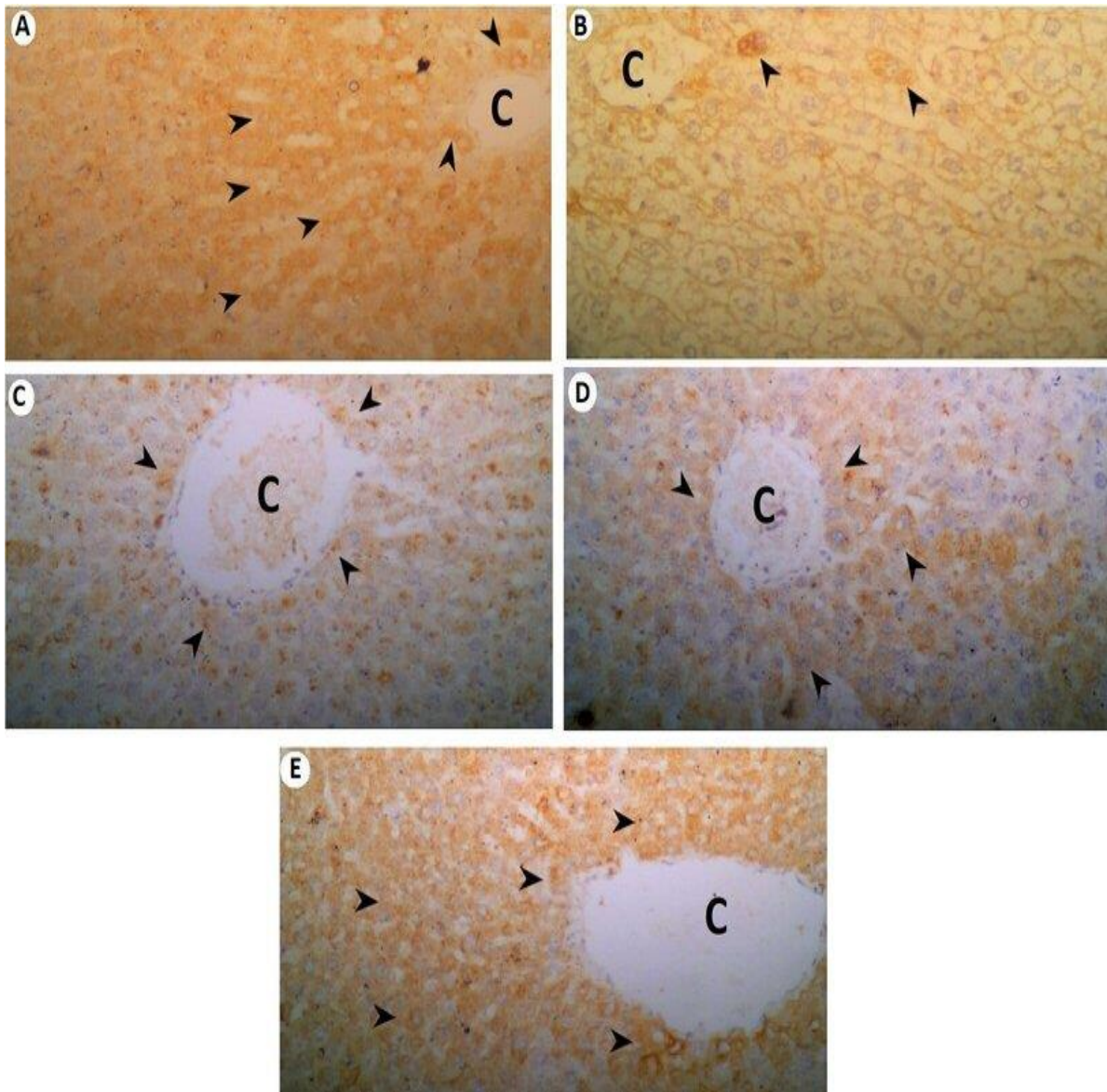


**Fig. (8):** Photomicrographs of rat hepatic sections of Bcl2 antibody immune stained showing: (A) group I, (B) group II, (C) group III, (D) group IV and (E) group V. According to the positive hepatocytes (head arrows), immunostaining was strong intense in groups I (A) and V (E); it was weaker in group II (B); and it returned to a moderate level in groups III and IV (C and D). A close neighbour to the central veins (C) were the reactive liver cells (head arrows). (Bcl2 antibody, X:400)

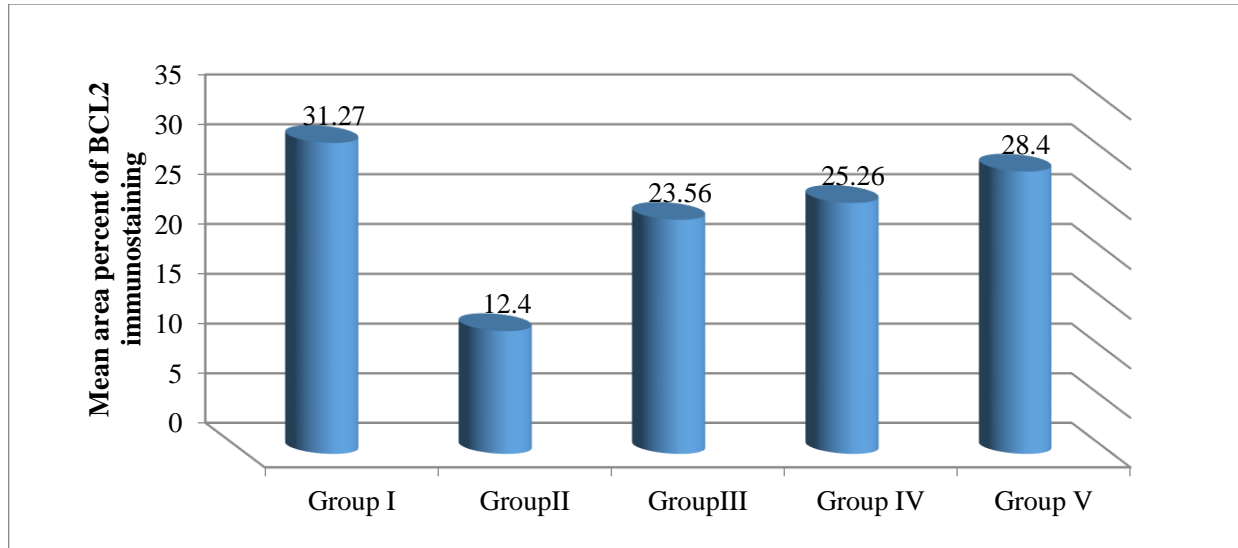


**Fig.9 : Comparison of area percent of positive reaction of Bcl-2 between different studied groups**

**BAX** Anti-Bax antibody immunostained liver tissue from control rats revealed its absence in the cytoplasm of hepatocytes. (Fig.10a). While liver sections from rats of group II showed patches of hepatic tissue with strong positive immunostaining (Fig.10b). The liver sections from rats of group III and IV showed remarkable decrease of the immunostained hepatic tissue surrounding the central vein (Figs.10c-e). Meanwhile, Group V only showed very little anti-Bax immunoreactivity around the blood sinusoids' edges. Liver from rats of group I, III, IV and V showed a significant decrease ( $p<0.05$ ) in the expression of anti Bax antibody as compared to group II (table 2, Fig.11).

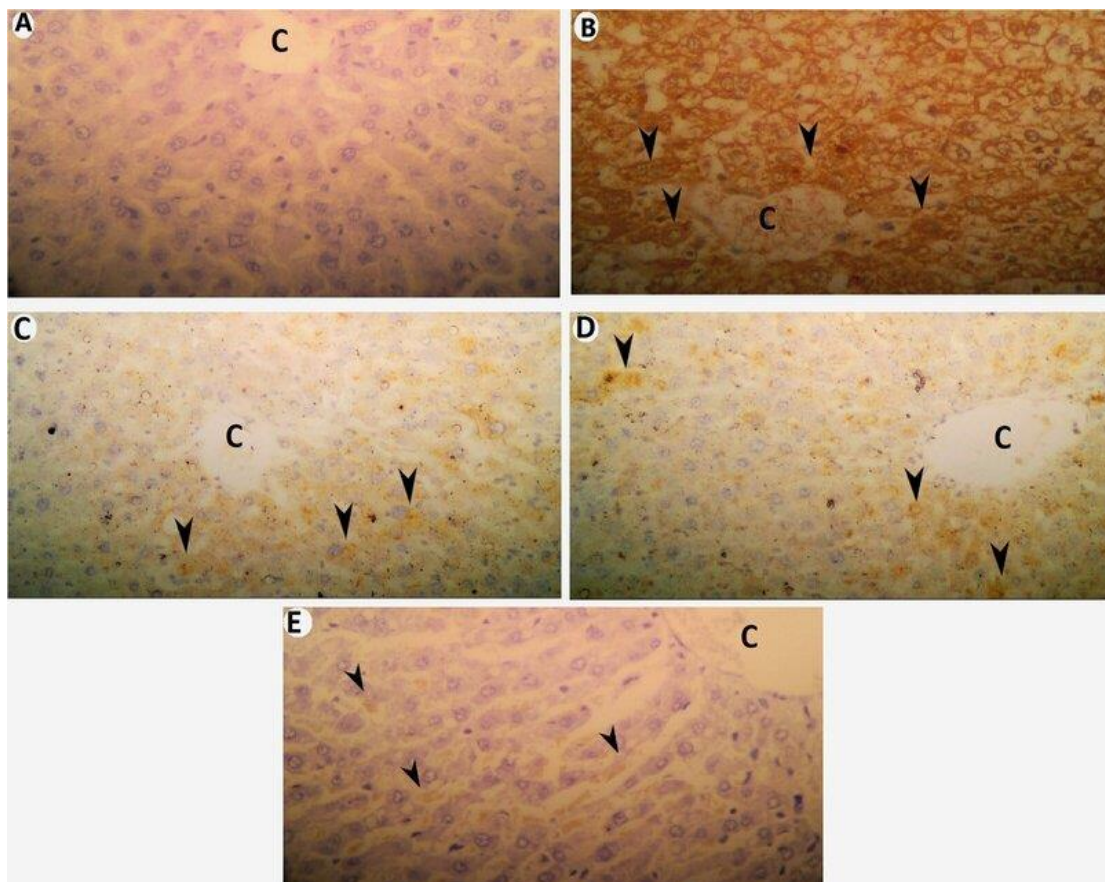


**Fig. (10): Photomicrographs of rat hepatic sections of anti-Bax antibody immune stained: (A) group I, (B) group II, (C) group III, (D) group IV and (E) group V. No colour is seen in hepatic section of Group I. In Group II, the Bax protein is expressed in the cytoplasm of hepatocytes (head arrows) near the central vein (c). This protein is less noticeable (head arrows) in groups III and IV than it is in group II. Group V only exhibited mild anti-Bax immunoreactivity (head arrows) around the hepatic blood sinusoids' edges. ( anti-Bax antibody, X:400).**

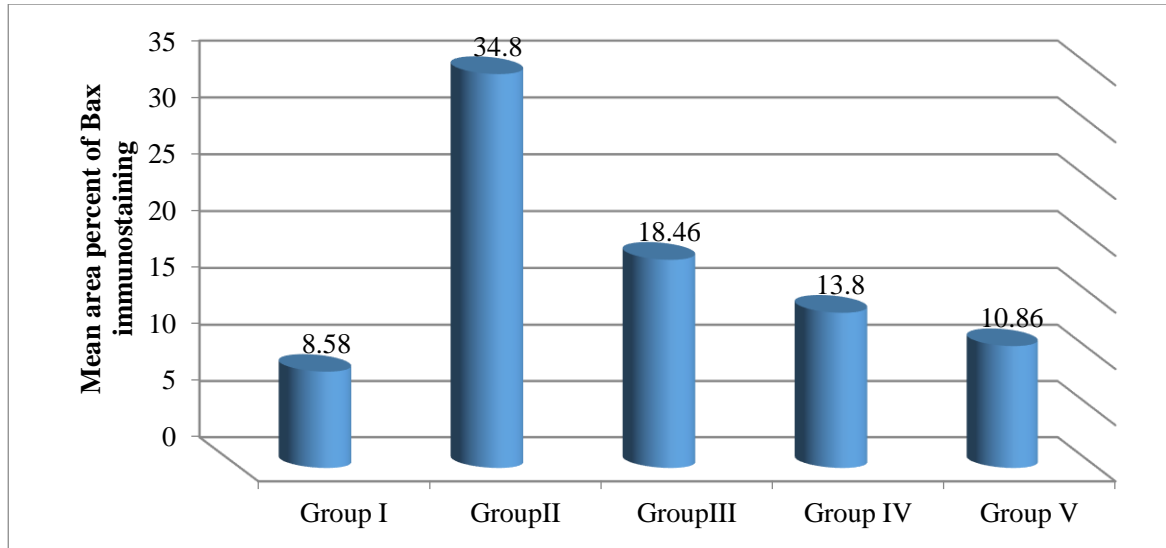


**Fig. 11: Comparison of area percent of positive reaction of Bax between different studied groups**

**Table (2): Comparison of area percent of positive reaction of Bcl-2 and Bax between different studied groups**

Mean % ± SD	Group I	Group II	Group III	Group IV	Group V
<b>BCL2</b>	31.27±4.5 <sup>P</sup>	12.4±0.98 <sup>c,R,U&amp;T</sup>	23.56±1.2 <sup>P</sup>	25.26±1.3 <sup>P</sup>	28.4±2.3 <sup>P</sup>
<b>Bax</b>	8.58 ± 2.1 <sup>P</sup>	34.8 ± 5.8 <sup>c,R,U&amp;T</sup>	18.46 ± 2. 8 <sup>P</sup>	13.8 ± 2.4 <sup>P</sup>	10.86 ± 2.1 <sup>P</sup>

The value of groups is presented as mean±SD.: significance <0.05.

c: Significance vs group I, p: Significance vs group II, R: Significance vs group III, U: Significance vs group IV, T: Significance vs group V.

## DISCUSSION

One million people die each year from liver disease, which is a worldwide public health burden <sup>(18)</sup>. According to **Papay et al.** <sup>(19)</sup>, a number of etiological variables, including hepatotoxins chemical exposure, metabolic disorders, and drinking, contribute to liver injury, which frequently results in severe necrosis. The adverse effects and intrinsic toxicities of the currently available medications make it challenging to treat hepatotoxicity. Finding a safe and efficient alternative to handle liver treatment is thus important. The hepatoprotective medication should be able to restore the liver's natural architecture and maintain the normal physiological systems that the hepatotoxins have altered <sup>(13)</sup>. Therefore, in this study, the CCl<sub>4</sub>'s hepatotoxic effects and the protective effects of riboflavin and Urolithin A on it were investigated.

In this study, the liver toxicity was verified by the intraperitoneal injection of CCl<sub>4</sub>, which caused a significant increase in ALT and AST activity. These enzymes generally reside in the cytoplasm due to increased cellular membrane permeability brought on by toxicity. When the liver is damaged, they can reach the bloodstream <sup>(20)</sup>. Additionally, some researchers report that after receiving CCl<sub>4</sub> these enzyme activities significantly increase. <sup>(1, 21)</sup>. As shown by lower blood ALT and AST levels, treatment of experimental rats with riboflavin alone, Urolithin A alone, or a combination of both medications exhibited a significant protective effect against CCl<sub>4</sub>-induced hepatotoxicity in rats. Riboflavin <sup>(13)</sup> and Urolithin A <sup>(12, 22)</sup> have both been proven to have

a hepatoprotective effect in animal models of acute liver damage. In the current study, Hepatocytes were disturbed and vacuolated; according to histopathological alterations seen in the liver of administered CCl<sub>4</sub> rats. Severe vacuolization was evident, along with extensive necrosis and degeneration. These results are similar to the previous reports, which showed marked cell necrosis, loss of liver cell architecture, and the formation of fat droplets in mice treated with CCl<sub>4</sub>. Cell disintegration and condensed nuclei were present <sup>(23)</sup>.

According to a prior study, CCl<sub>4</sub> injection causes the cytochrome system to become activated and produce trichloromethyl radicals, which are known to cause oxidative stress and lipid peroxidation <sup>(24)</sup>. According to **Vulimiri et al.** <sup>(25)</sup>, apoptosis or necrosis of liver tissues develops in large part due to CCl<sub>4</sub>-induced oxidative stress. Cells have created a detoxification and antioxidant defence mechanism, comprising enzymatic (like CAT and GSH-Px) and nonenzymatic antioxidants like glutathione, to protect themselves against toxic damages and the harm caused by oxygen-free radicals. All flavoproteins, including glutathione reductase, which shields cells from the damaging effects of ROS, need it since it is the main building block of the cofactors flavin adenine dinucleotide (FAD) and flavin mononucleotide (FMN) <sup>(26)</sup>. The activation of Kupffer cells in the liver caused by enhanced oxidative damage caused by CCl<sub>4</sub> derivatives may also be the cause of increased TNF-release from inflammatory cells drawn to the liver. By preventing leukocytes from releasing the



proinflammatory cytokine TNF-, riboflavin protected the liver from damage brought on by CCl<sub>4</sub> (13).

In this study, Rats administered CCl<sub>4</sub> and treated with riboflavin alone displayed tiny foci of hepatic cells with minimal cellular damage and cellular infiltrations. **Al-Harbi et al.** (13) revealed a similar improvement in liver function, inflammatory biomarkers, and histological results in riboflavin-administered groups. This idea was further corroborated by **Li et al.** (27) and **Sanches et al.** (28), who discovered that riboflavin supplementation significantly decreased liver tissue damage and enhanced oxidative stress indicators (GSH, SOD) and liver function biomarkers (AST, ALT) in a rat model. Rats given CCl<sub>4</sub> and treated with Urolithin A alone most hepatocytes with normal cytoplasm and minimal cellular infiltration. The present findings are confirmed by earlier research by **Karim et al.** (12), who noted that the vacuolization and inflammatory cells of the Doxorubicin with Urolithin A (5 mg/kg) treatment group significantly improved, but necrosis showed only a minor improvement. Since numerous studies found reduced production of TNF- and IL-6, two important inflammatory cytokines, Urolithin A's anti-inflammatory effect may have contributed to the reported hepatoprotective advantages in this study (22, 29, 30). In this work, Masson's trichrome stain revealed that, in comparison to other groups, the CCl<sub>4</sub> group exhibited a more concentrated distribution of collagen fibers around central vein and the portal area. This result was in line with the research (17) done in rat models of alphanaphthylisothiocyanate-induced toxicity. However, **Fadda et al.** (31) found no changes in liver sections stained with Mason trichrome between either of the treatment groups or the acetaminophen toxicity rat model, confirming the absence of fibrosis.

The Bax protein has a significant impact on how cell apoptosis is regulated. Cell death may result from high levels of Bax expression and the synthesis of homo- or heterodimers with Bcl-2. Bax is clearly expressed at 24-72 h after reperfusion, as previously shown (32). In this study, histomorphometric analysis of the immunohistochemistry sections may indicate an increase of pro-apoptotic proteins (Bax) and a downregulation of anti-apoptotic proteins (Bcl2) at the seventh day of administration of CCl<sub>4</sub> in rat models. This was in agreement with some researchers who showed that elevated Bax expression and apoptotic index in a rat model of titanium dioxide-induced hepatotoxicity, Acetaminophen induced hepatotoxicity and acrylamide-induced hepatotoxicity (15, 31, 33).

The considerable downregulation of pro-apoptotic Bax and the significant elevation of anti-apoptotic protein, Bcl2, may be attributable to either riboflavin alone or urolithin A alone. These findings were in line with those of other research on the anti-hepatotoxic properties of riboflavin (13) and urolithin A (12) in rat models. Additionally, riboflavin shortage accelerated the rate of cell death, increased the expression of proapoptotic indicators (Bax), and lowered

the expression of antiapoptotic markers (Bcl2). (34). In CCl<sub>4</sub> administered group and treated with Riboflavin and Urolithin A combination, improved liver enzymes were in accord with the repaired hepatic structural organization with no cellular infiltrations. The immunoassay slides' morphometric analysis indicated that the results were better to those of single treatments. Due to the further inclusion of the antioxidant and anti-inflammatory effects, these findings alluded to the summative activities of both riboflavin and urolithin A.

## CONCLUSION

In currently used rat model of CCl<sub>4</sub> exposure, carbon tetrachloride hepatotoxicity was demonstrated. The biochemical and histological data pointed to a considerable modification in the hepatic tissues that triggered oxidative stress and inflammation. Urolithin and Riboflavin are only given once. Strong anti-inflammatory and antioxidant benefits were seen after therapy. When given together, they had stronger synergistic effects and boosted the antioxidant capacity.

## Conflict of interest

There are no stated conflicts of interest by the authors.

## REFERENCES

1. **Noumi V, Deli M, Nguimbou R et al. (2022):** Particle size effects on antioxidant and hepatoprotective potential of essential oil from eucalyptus camaldulensis leaves against carbon tetrachloride-induced hepatotoxicity in rats. *Pharmacology & Pharmacy*, 13(08): 253-272.
2. **Zhang Y, Zhou J, Liu J et al. (2021):** RNA-Seq analysis of the protection by *Dendrobium nobile* alkaloids against carbon tetrachloride hepatotoxicity in mice. *Biomedicine & Pharmacotherapy*, (137): 111307-1113118.
3. **Aslan A, Gok O, Beyaz S et al. (2020):** Ellagic acid prevents kidney injury and oxidative damage via regulation of Nrf-2/NF-κB signaling in carbon tetrachloride induced rats. *Molecular biology reports*, (47): 7959-7970
4. **Combs G, McClung J (2017):** Riboflavin, in *The Vitamins*, Elsevier: 315-329. <https://shop.elsevier.com/books/the-vitamins/combs-jr/978-0-12-802965-7>
5. **Alhazza I, Hassan I, Ebaid H et al. (2020):** Chemopreventive effect of riboflavin on the potassium bromate-induced renal toxicity in vivo. *Naunyn-Schmiedeberg's archives of pharmacology*, 393(12): 2355-2364.
6. **Al-Harbi N, Imam F, Nadeem A et al. (2015):** Riboflavin attenuates lipopolysaccharide-induced lung injury in rats. *Toxicology mechanisms and methods*, 25(5): 417-423.
7. **Karakoyun B, Ertaş B, Yüksel M et al. (2018):** Ameliorative effects of riboflavin on acetic acid-induced colonic injury in rats. *Clinical and experimental pharmacology & physiology*, 45(6): 563-572.
8. **Espín J, Larrosa M, García-Conesa M et al. (2013):** Biological significance of urolithins, the gut microbial ellagic Acid-derived metabolites: the evidence so far. *Evidence-based complementary and alternative medicine*, 2013:270418
9. **Luan P, D'Amico D, Andreux P et al. (2012):** Urolithin A improves muscle function by inducing mitophagy in muscular dystrophy. *Science translational medicine*, 13(588): eabb0319.
10. **Albasher G, Alkahtani S, Al-Harbi L (2022):** Urolithin A prevents streptozotocin-induced diabetic cardiomyopathy in rats by activating SIRT1. *Saudi journal of biological sciences*, 29(2): 1210-1220.
11. **Bertollo C, Oliveira A, Rocha L et al. (2006):** Characterization of the antinociceptive and anti-inflammatory activities of riboflavin in different experimental models. *European journal of pharmacology*, 547(1-3): 184-191.

12. **Karim S, Madani B, Burzangi A et al. (2023):** Urolithin A's Antioxidative, Anti-Inflammatory, and Antiapoptotic Activities Mitigate Doxorubicin-Induced Liver Injury in Wistar Rats. **Biomedicines, 11(4): 1125- 1135.**
13. **Al-Harbi N, Imam F, Nadeem A et al. (2014):** Carbon tetrachloride-induced hepatotoxicity in rat is reversed by treatment with riboflavin. **International immunopharmacology, 21(2): 383–388.**
14. **Bancroft J, Layton C (2019):** The Hematoxylin and Eosin /Connective and other mesenchymal tissues with their stains. In: Suvarna KS, Layton C, Bancroft JD (eds.), Bancroft's theory and practice of histological techniques E-Book. 8th ed. Elsevier Health Sciences.
15. **Orazizadeh M, Khorsandi L, Mansouri E et al. (2020):** The effect of glycyrrhizin acid on Bax and Bcl2 expression in hepatotoxicity induced by Titanium dioxide nanoparticles in rats. **Gastroenterology and Hepatology from Bed to Bench, 13(2): 168- 176.**
16. **Krishna M (2013):** Role of special stains in diagnostic liver pathology. **Clinical liver disease, 2(1): S8–S10.**
17. **Badr A, Farid M, Biomy A et al. (2020):** Protective effect of Toxocara vitulorum extract against alpha-naphthylisothiocyanate-induced cholangitis in rat. **JoBAZ., 81 (62): 197-202.**
18. **Xiao J, Wang, F, Wong N et al. (2019):** Global liver disease burdens and research trends: Analysis from a Chinese perspective. **Journal of hepatology, 71(1): 212–221.**
19. **Papay J (2009):** Response to Letter to the editor by Papay: Regulatory Toxicology and Pharmacology 54 (2009): 84-90. Drug-induced liver injury following positive drug rechallenge. **Regulatory Toxicology and Pharmacology, 54(3):314-314.**
20. **Cherubini A, Ruggiero, C, Polidori M et al. (2005):** Potential markers of oxidative stress in stroke. **Free radical biology & medicine, 39(7): 841–852.**
21. **Popoola A, Ademilusi E, Adedeji T et al. (2022):** Effect of silymarin on blood coagulation profile and osmotic fragility in carbon tetrachloride induced hepatotoxicity in male Wistar rats. **Toxicology reports, (9): 1325–1330.**
22. **Gao Z, Yi W, Tang J et al. (2022):** Urolithin A protects against acetaminophen-induced liver injury in mice via sustained activation of Nrf2. **International journal of biological sciences, 18(5): 2146–2162.**
23. **Dai C, Li H, Wang Y et al. (2021):** Inhibition of Oxidative Stress and ALOX12 and NF-κB Pathways Contribute to the Protective Effect of Baicalein on Carbon Tetrachloride-Induced Acute Liver Injury. **Antioxidants (Basel, Switzerland), 10(6): 976-980.**
24. **Wills P and Asha V (2006):** Protective effect of Lygodium flexuosum (L.) Sw. extract against carbon tetrachloride-induced acute liver injury in rats. **Journal of ethnopharmacology, 108(3): 320–326.**
25. **Vulimiri S, Berger A, Sonawane B (2011):** The potential of metabolomic approaches for investigating mode(s) of action of xenobiotics: case study with carbon tetrachloride. **Mutation research, 722(2): 147–153.**
26. **Depeint F, Bruce W, Shangari N et al. (2006):** Mitochondrial function and toxicity: role of the B vitamin family on mitochondrial energy metabolism. **Chemico-biological interactions, 163(1-2): 94–112.**
27. **Li D, Song Y, Wang Y et al. (2020):** Nos2 deficiency enhances carbon tetrachloride-induced liver injury in aged mice. **Iranian journal of basic medical sciences, 23(5): 600–605.**
28. **Sanches S, Ramalho L, Mendes-Braz M et al. (2014):** Riboflavin (vitamin B-2) reduces hepatocellular injury following liver ischaemia and reperfusion in mice. **Food and chemical toxicology : an international journal published for the British Industrial Biological Research Association, 67: 65–71.**
29. **Chen Y, Hua Y, Li X et al. (2020):** Distinct Types of Cell Death and the Implication in Diabetic Cardiomyopathy. **Frontiers in pharmacology, 11: 42.**
30. **Fiordelisi A, Iaccarino G, Morisco C et al. (2019):** NfκappaB is a Key Player in the Crosstalk between Inflammation and Cardiovascular Diseases. **International journal of molecular sciences, 20(7): 1599-1616.**
31. **Fadda L, Al-Rasheed N, Hasan I et al. (2017):** Bax and CD68 expression in response to liver injury induced by acetaminophen: the hepatoprotective role of thymoquinone and curcumin. **Pakistan journal of Zoology, 49(1): 85-93.**
32. **Liu G, Wang T, Wang T et al. (2013):** Effects of apoptosis-related proteins caspase-3, Bax and Bcl-2 on cerebral ischemia rats. **Biomedical reports, 1(6): 861-867.**
33. **Sayed S, Alotaibi S, El-Shehawi A et al. (2022):** The anti-inflammatory, anti-apoptotic, and antioxidant effects of a pomegranate-peel extract against acrylamide-induced hepatotoxicity in rats. **Life, 12(2): 224-232.**
34. **Zhang B, Cao J, Wu Y et al. (2022):** Riboflavin (Vitamin B2) Deficiency Induces Apoptosis Mediated by Endoplasmic Reticulum Stress and the CHOP Pathway in HepG2 Cells. **Nutrients, 14(16): 3356-3364.**